scientific reports

Check for updates

OPEN

Targeted inhibition of glycogen synthase kinase-3 using 9-ING-41 (elraglusib) enhances CD8 T-cell-reactivity against neuroblastoma cells

A. Markovska[1], K. Somers[2,3], J. Guillaume[1], J. Melief[4], A. P. Mazar[5], D. M. Schmitt[5], H. S. Schipper[1,6] & M. Boes[1,7]✉

The prognosis of patients with high-risk neuroblastoma remains poor, partly due to inadequate immune recognition of the tumor. Neuroblastomas display extremely low surface MHC-I, preventing recognition by cytotoxic T lymphocytes (CTLs) and contributing to an immunosuppressive tumor microenvironment. Glycogen synthase kinase-3 beta (GSK-3β) is involved in pathways that may affect the MHC-I antigen processing and presentation pathway. We proposed that therapeutic inhibition of GSK-3β might improve the surface display of MHC-I molecules on neuroblastoma cells, and therefore tested if targeting of GSK-3β using the inhibitor 9-ING-41 (Elraglusib) improves MHC-I-mediated CTL recognition. We analyzed mRNA expression data of neuroblastoma tumor datasets and found that non-MYCN-amplified neuroblastomas express higher GSK-3β levels than MYCN-amplified tumors. In non-MYCN-amplified cells SH-SY5Y, SK-N-AS and SK-N-SH 9-ING-41 treatment enhanced MHC-I surface display and the expression levels of a subset of genes involved in MHC-I antigen processing and presentation. Further, 9-ING-41 treatment triggered increased STAT1 pathway activation, upstream of antigen presentation pathways in two of the three non-MYCN-amplified cell lines. Finally, in co-culture experiments with CD8+T cells, 9-ING-41 improved immune recognition of the neuroblastoma cells, as evidenced by augmented T-cell activation marker levels and T-cell proliferation, which was further enhanced by PD-1 immune checkpoint inhibition. Our preclinical study provides experimental support to further explore the GSK-3β inhibitor 9-ING-41 as an immunomodulatory agent to increase tumor immune recognition in neuroblastoma.

Keywords Neuroblastoma, GSK-3β, Immunomodulation, MHC-I

Abbreviations

CTLs	Cytotoxic T lymphocytes
GSK-3β	Glycogen synthase kinase-3 beta
APM	Antigen presentation machinery
PRC2	Polycomb repressive complex 2
HLA	Human leukocyte antigen
PSMB8	Proteasome 20S subunit B8
TAP1	Transporter associated with antigen processing 1
TAP2	Transporter associated with antigen processing 2
CTV	Cell trace violet

[1]Center for Translational Immunology, University Medical Center Utrecht, Utrecht University, Heidelberglaan 100, 3508 GA Utrecht, The Netherlands. [2]Lowy Cancer Research Centre, Children's Cancer Institute, UNSW Sydney, Sydney, NSW, Australia. [3]School of Clinical Medicine, UNSW Sydney, Sydney, NSW, Australia. [4]Karolinska Institutet, Stockholm, Sweden. [5]Actuate Therapeutics, Fort Worth, TX 76107, USA. [6]Pediatric Cardiology, Sophia Children's Hospital, Erasmus Medical Centre, Rotterdam, The Netherlands. [7]Department of Pediatrics, University Medical Center Utrecht, Utrecht, Heidelberglaan 100, 3508 GA, The Netherlands. ✉email: M.L.Boes@umcutrecht.nl

STAT1 Signal transducer and activator of transcription 1
NK cell Natural killer cells

Neuroblastoma is an embryonic tumor originating from neural crest precursor cells, and is the third most prevalent pediatric solid tumor. The estimated five-year progression free survival of high-risk neuroblastoma patients remains in the range of 50–60%[1]. *MYCN* amplification is a strong marker of poor prognosis and is present in approximately 20% of neuroblastomas.

In the last decade immunotherapy has gained significant traction for the treatment of neuroblastoma. Monoclonal anti-GD2 is now incorporated in first-line and relapse treatment protocols for patients with neuroblastoma[2]. The working mechanism of anti-GD2 monoclonal antibody therapy is through antibody-mediated tumor cell killing. As an alternative therapeutic approach, cytotoxic T lymphocyte (CTL)-mediated killing is being considered. Specifically, peptide centric PHOX2B chimeric antigen receptor (CAR) T cell-based therapies have recently shown promising results in specific killing of neuroblastoma cells in vitro and potent tumor regression in mice[3]. However, the exploitation of T-cell-based immunotherapy for neuroblastoma has been hampered as these tumors usually express extremely low levels of peptide/MHC-I complexes[4]. MHC-I surface display is critical for CTLs to recognize and mount responses against transformed or infected cells. It was already established that neuroblastoma cells can be recognized by CTLs when MHC-I-mediated antigen presentation is restored[4]. In addition to MHC-I, other components of the antigen presentation machinery (APM) can also be repressed in tumors[5,6]. For example, it was shown that reduced expression of MHC-I in neuroblastoma is caused by silencing of APM proteins, as mediated by a transcriptional repressor complex, polycomb repressive complex 2 (PRC2)[7]. We considered the possibility that CTL-based cellular therapy might be improved when combined with a targeted cancer drug that can augment the tumor display of peptide/MHC-I complexes. As such, in conditions of increased presentation of tumor-specific peptide/MHC-I complexes, checkpoint inhibitor treatment might further improve anti-tumor CTL cellular therapies.

Glycogen synthase kinase-3β (GSK-3β), a serine/threonine kinase which is currently under investigation as a target in cancer therapies based on its important role in many essential cellular processes, has also been shown to impact several important pathways that regulate the MHC-I antigen processing and APM, i.e., IFNγ mediated signaling[8–10] and the NF-κB pathway[11–14]. Moreover, polycomb proteins are downstream targets of GSK-3β signaling[15,16], indicating that GSK-3β activity might contribute to APM silencing. Furthermore, GSK-3β is active in neuroblastoma and has been identified as a positive regulator of NF-κB-mediated survival and chemoresistance in neuroblastoma cells[17,18].

In this study, we explored whether 9-ING-41 (Elraglusib), a small molecule inhibitor of GSK-3β that is currently in clinical development, can modulate neuroblastoma cell presentation of peptide/MHC-I complexes. Thus far, GSK-3β inhibition using 9-ING-41 has been shown to decrease neuroblastoma cell survival via suppression of NF-κB-driven BCl-2 and XIAP expression[18–21]. In the current work, we show a new feature of pharmacological inhibition of GSK-3β with 9-ING-41, namely the enhancement of immune recognition of non-MYCN amplified neuroblastoma cells by CTLs.

Results

Increased GSK-3β gene expression is associated with reduced survival of patients with non-MYCN-amplified neuroblastoma

It is well-established that enhanced GSK-3β activity supports survival, proliferation, and treatment resistance in many cancers. To evaluate the role for the pathway in neuroblastoma, we first assessed GSK-3β expression levels in the Cancer Cell Line Encyclopedia (Broad, 2019) using the cBioPortal database[22–25]. We found that cell lines derived from neuroblastomas were among the highest GSK-3β expressing cancer cell lines (Fig. 1a).

Although GSK-3β is found to be highly expressed in the majority of neuroblastomas[18], the association between GSK-3β expression and survival of patients with neuroblastoma is unexplored. To this end, we investigated the Seeger (102 neuroblastoma patients) and Versteeg (88 neuroblastoma patients) datasets, using the publicly available R2 genomics analysis and visualization platform (AMC, the Netherlands). We used the automatically generated GSK-3β expression cutoff values based on statistically significant differences using log-rank test and with minimum group size of 30. High GSK-3β expression significantly correlated with worse event-free survival in the Seeger but not in the Versteeg cohort (Fig. 1b, c). As the Seeger cohort only contains non-MYCN-amplified neuroblastoma patients, while the Versteeg cohort contains both MYCN-amplified and non-MYCN amplified patients, we next looked separately at the prognostic relevance of GSK-3β expression in these two neuroblastoma subtypes in the Versteeg cohort. While no significant associations were detected between GSK-3β expression and outcome in any of the subgroups, a trend was observed for a link between high GSK-3β expression and poor outcome in the non-MYCN-amplified tumors (Fig. 1d, e).

Further, we compared the GSK-3β expression levels in MYCN-amplified versus non-MYCN-amplified neuroblastomas from the TARGET cohort of 143 patients, using the cBioPortal database[22–24] and the Versteeg cohort (described above). Neuroblastomas without MYCN amplification had significantly higher GSK-3β expression compared to MYCN-amplified neuroblastomas in the TARGET cohort (Fig. 1f). Further, we also observed a trend where the non-MYCN-amplified tumors had higher GSK-3β expression compared to MYCN-amplified tumors in the Versteeg cohort, however this difference did not reach statistical significance (Fig. S1). Overall, our data indicate that GSK-3β is more expressed in neuroblastomas without MYCN amplification and that, primarily in the neuroblastoma patients without MYCN amplification, GSK-3β expression correlates negatively with survival.

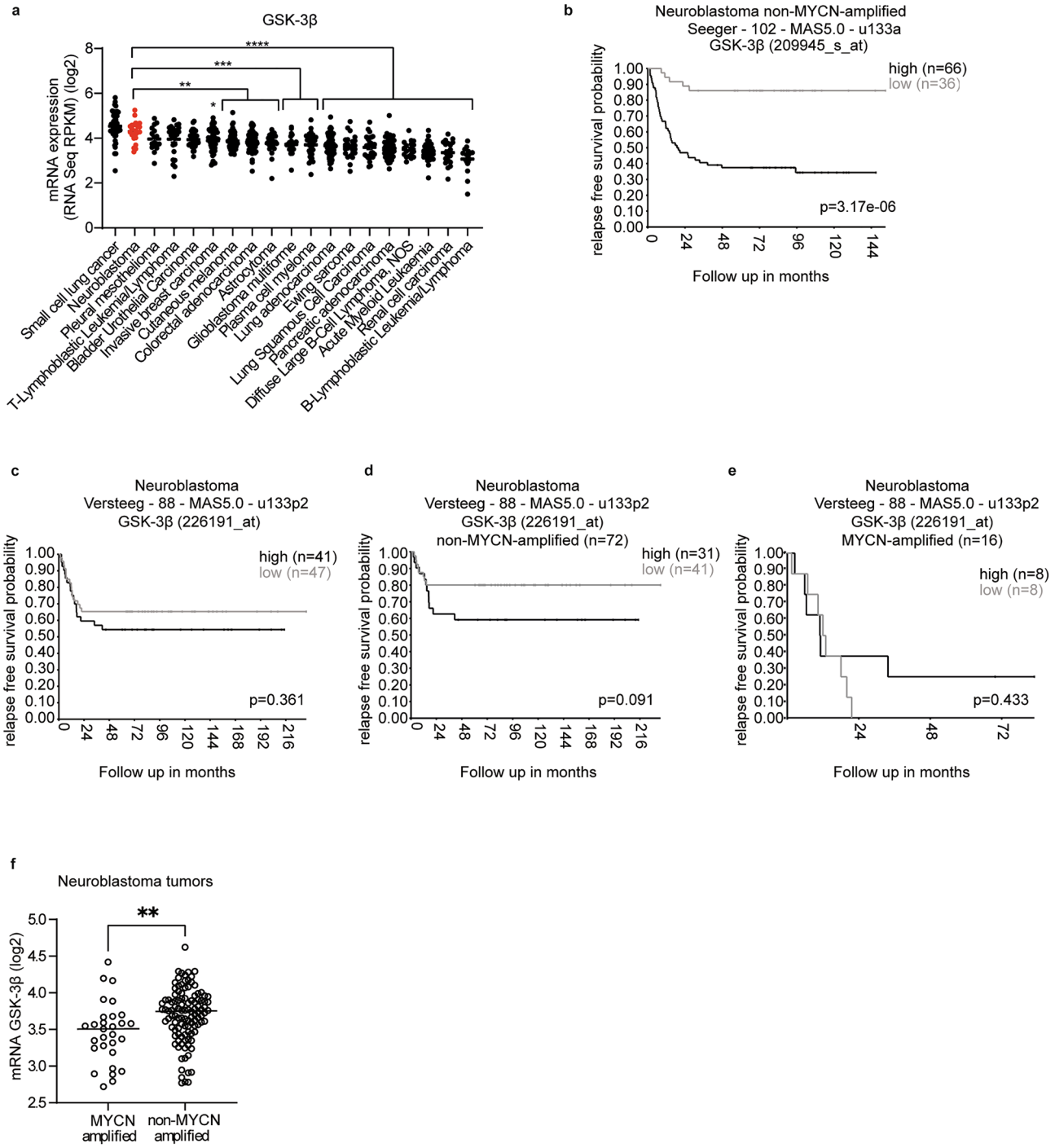

Fig. 1. Association of GSK-3β expression level on tumor cells with survival of patients with neuroblastoma. (**a**) GSK-3β expression levels among different tumor cell lines in the Cancer cell line Encyclopedia (Broad, 2019) available on the cBioPortal database. One-way ANOVA with Dunnett's multiple comparison test, where*$p<0.05$, **$p<0.01$, ***$p<0.001$ ****$p<0.0001$ was used to compare the expression of GSK-3β in neuroblastoma cells to other cancer cell lines. The expression levels of GSK-3β were correlated with survival of patients with neuroblastoma from two cohorts, Seeger (**b**) and Versteeg (**c**). The Seeger cohort contains only non-MYCN amplified neuroblastomas. The Versteeg cohort contains both MYCN-amplified and non-amplified tumors, and we also looked at the non-MYCN amplified (**d**) and MYCN-amplified (**e**) tumors from the cohort separately. Log-rank test was used, $p<0.05$ was considered significant. (**f**) GSK-3β expression in MYCN-amplified and non-amplified neuroblastoma tumors from the TARGET cohort of 143 patients (cBioPortal database). GSK-3β, glycogen synthase kinase-3 beta.

9-ING-41 can enhance MHC-I display on neuroblastoma cells

Based on its involvement in immune modulation, we hypothesized that GSK-3β activity may be involved in the characteristically low expression of MHC-I molecules in neuroblastoma tumors[26]. We used the STRING database to gain greater insight into the possible interactions of GSK-3β with proteins involved in MHC-I antigen processing and presentation. GSK-3β may interact with proteins involved in MHC-I-mediated antigen processing and presentation and the IFNγ-signaling pathway (Fig. 2a), which is a strong inducer of multiple genes that are part of the MHC-I antigen processing and presentation machinery (APM)[4,27] and is known to enhance MHC-I expression on neuroblastoma cells[28,29]. We hypothesized that as GSK-3β associated with MHC-I APM, its inhibition might invigorate MHC-I signaling in the lowly immunogenic neuroblastoma tumors.

To test the possibility that GSK-3β acts as a regulator of MHC-I-mediated antigen presentation in neuroblastoma, we made use of a small molecule GSK-3β inhibitor, 9-ING-41, that was previously shown to inhibit GSK-3β activity in neuroblastoma cells[18]. We used IMR-32 and SK-N-BE(2) as representative MYCN-amplified neuroblastoma cell lines, and SH-SY5Y, SK-N-SH and SK-N-AS as representative non-MYCN-amplified neuroblastoma cell lines (Fig. 2b)[30,31]. In support of our findings in neuroblastoma patients (Fig. 1f), two out of three non-MYCN-amplified cell lines expressed significantly more GSK-3β mRNA compared to the MYCN-amplified neuroblastoma cells (Fig. 2c).

We treated the neuroblastoma cells with 9-ING-41 at a concentration of 100 nM previously shown to effectively suppress the activity of GSK-3β in neuroblastoma cells[18]. As GSK-3β inhibition by itself might not be sufficient to induce MHC-I upregulation, we also exposed neuroblastoma cells to a combination of IFNγ, a known inducer of MHC-I expression, and 9-ING-41. We analyzed the viable cells for surface MHC-I expression with a pan-MHC-I antibody using flow cytometry. 9-ING-41 treatment significantly increased MHC-I surface expression on the IMR-32, SH-SY5Y and SK-N-AS cells but not on the SK-N-BE(2) and SK-N-SH cells (Fig. 2d, e).

When cultured in the presence of IFNγ, MHC-I expression increased in all cell lines, but it was not significantly further augmented by 9-ING-41 addition in the MYCN-amplified cells (Fig. 2d). However, MHC-I cell surface expression was significantly enhanced by 9-ING-41 addition in the conditions with IFNγ co-treatment in all non-MYCN-amplified cell lines we tested (Fig. 3e). To evaluate whether this phenomenon is specific for non-MYCN-amplified neuroblastoma, we assessed the effect of MYCN overexpression on MHC-I expression induction in the SH-SY5Y cells. SH-SY5Y cells that overexpressed MYCN (supplemental Fig. S2a) did not change GSK-3β expression levels (supplemental Fig. S2b). Correspondingly, sensitivity to 9-ING-41 treatment was retained, and the MYCN-overexpressing SH-SY5Y cells showed 9-ING-41 induced MHC-I upregulation in presence of IFNγ treatment (supplemental Fig. S2c).

Taken together, these results show that MHC-I display on neuroblastoma cells can be enhanced with singular 9-ING-41 treatment, and also in combination with IFNγ. These effects were most pronounced in the non-MYCN-amplified cells which were chosen to be the focus for subsequent experiments.

9-ING-41 can increase expression of genes involved in antigen processing and presentation in neuroblastoma cells

Next, we assessed whether GSK-3β inhibition affects the expression of components of the MHC-I APM. We treated the neuroblastoma cell lines with 9-ING-41 and/or IFNγ and measured the mRNA expression of key APM molecules Human Leukocyte Antigen (HLA)-B, proteasome 20S subunit B8 (PSMB8), Transporter Associated with antigen Processing 1 (TAP1) and TAP2 (Fig. 3a, b). We did not observe significant consistent differences in MHC-I mRNA expression, even though 9-ING-41 did increase the surface expression of MHC-I protein in all neuroblastoma cells tested, perhaps by MHC-I protein transfer from intracellular compartments (Fig. 2). All non-MYCN-amplified neuroblastoma cells cultured in the presence of 9-ING-41 expressed significantly increased mRNA levels of PSMB8 compared to conditions without 9-ING-41 (Fig. 3a, b). When analyzed for expression levels of the heterodimeric protein complex TAP1-TAP2, known to translocate short peptides from the cytosol into the ER to allow for peptide/MHC-I complex formation, we found that TAP1 was significantly upregulated in 9-ING-41-treated SH-SY5Y and SK-N-SH cells (Fig. 3a). However, there was no significant effect of 9-ING-41 treatment on TAP1 when cells were co-treated with IFNγ (Fig. 3b). TAP2 was significantly upregulated only in the SH-SY5Y cells co-treated with IFNγ (Fig. 3b). The expression of PSMB8, TAP1 and TAP2 in the MYCN-amplified IMR-32 and SK-N-BE(2) cell lines was not affected by 9-ING-41 treatment (supplemental Fig. S3).

In addition to the MHC-I APM pathway, GSK-3β may also interact with the IFNγ signaling pathway (Fig. 2a). As IFNγ signaling is known to upregulate MHC-I antigen processing and presentation[27], we also addressed whether GSK-3β inhibition may enhance IFNγ signaling in neuroblastoma cells. We measured the level of Signal Transducer and Activator of Transcription 1 (STAT1) expression after treating SH-SY5Y cells with 9-ING-41 and IFNγ. We found a significant mRNA increase of STAT1 in SH-SY5Y cells treated with combined 9-ING-41/IFNγ treatment when compared to IFNγ alone (Fig. 3c). There was no effect of 9-ING-41 treatment on STAT1 gene expression in the SK-N-AS (Fig. 3b) and SK-N-SH cells (Fig. S3). IFNγ signaling induces STAT1 phosphorylation. Next, we analyzed whether GSK-3β inhibition might enhance STAT1 phosphorylation. We used whole cell lysates from the non-MYCN-amplified cells SH-SY5Y, SK-N-AS and SK-N-SH stimulated with 9-ING-41 in the presence of IFNγ (30 min at 37 °C) for Western blotting. 9-ING-41 enhanced the amount of phosphorylated STAT1 in a dose-dependent manner in SH-SY5Y and SK-N-AS cells, but not in the SK-N-SH cells (Fig. 3d).

These data support that GSK-3β inhibition with 9-ING-41 may enhance antigen presentation by increasing the expression of genes encoding APM proteins, as contributed by enhanced IFNγ-mediated STAT1 signaling in neuroblastoma cells.

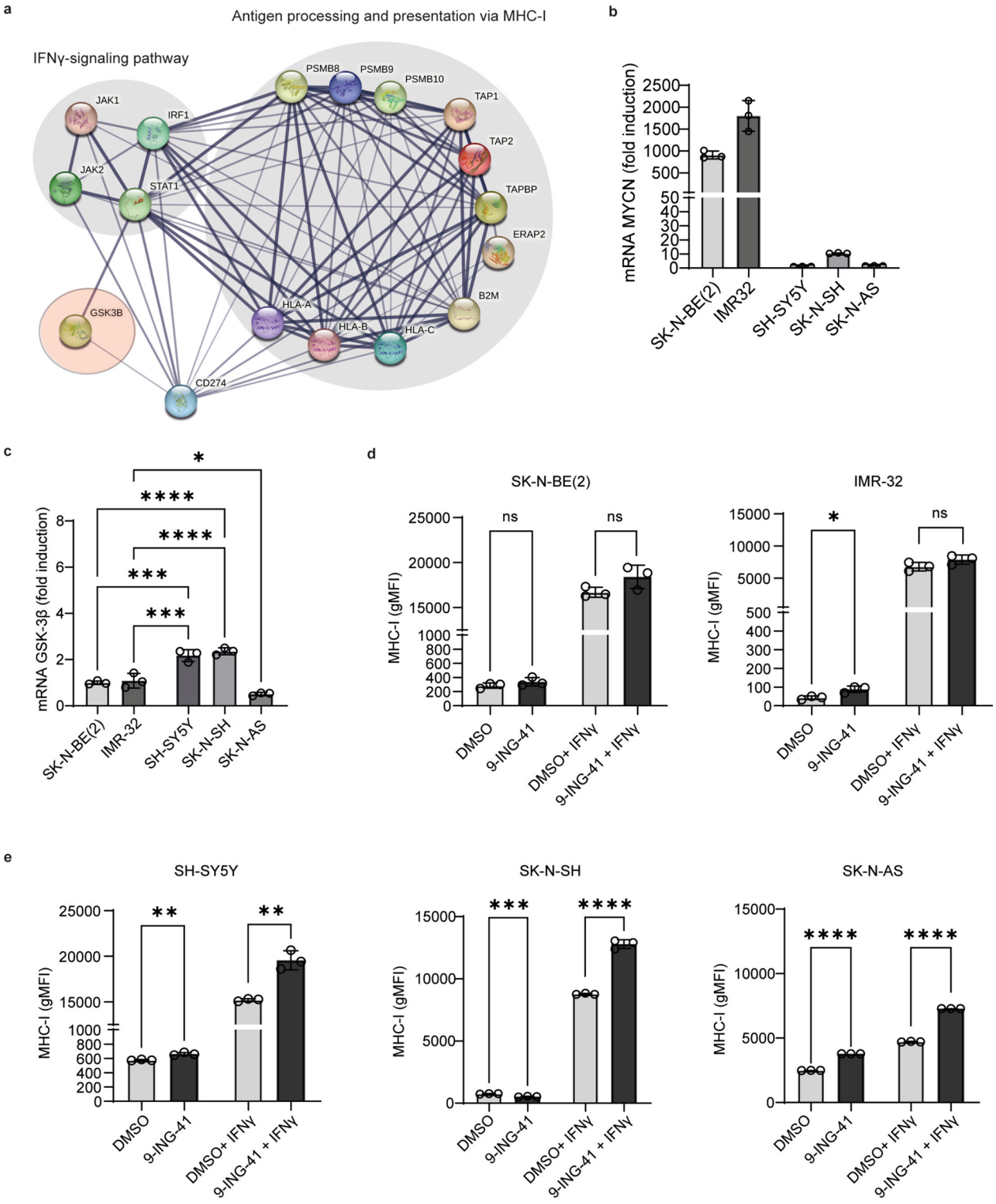

Fig. 2. GSK-3β inhibition with 9-ING-41 increases MHC-I cell surface expression on non-MYCN-amplified neuroblastoma cells. (**a**) Protein–protein interaction analysis of GSK-3β with proteins involved in MHC-I mediated antigen presentation and IFNγ signaling. The nodes indicate proteins, and edges indicate the number of interactions. Color saturation of the edges represents the confidence score of a functional association. Data obtained from STRING database. (**b**) MYCN mRNA expression across the neuroblastoma cell lines normalized on GAPDH expression and fold induction is shown relative to SH-SY5Y. (**c**) GSK-3β mRNA expression across neuroblastoma cell lines. Data are normalized to GAPDH expression and shown relative to SK-N-BE(2) cell line. $^{*}p<0.05$, $^{**}<0.01$, $^{***}<0.001$, $^{****}p<0.0001$ using one-way ANOVA with Šidák correction for multiple comparisons. MHC-I cell surface expression measured on flow cytometry on MYCN-amplified neuroblastoma cells SK-N-BE(2) and IMR-32 (d) and non-MYCN-amplified cells SH-SY5Y, SK-N-AS and SK-N-SH (e). Cells were treated for 72h with DMSO, 9-ING-41 (100 nM) or IFNγ (25 µg/ml) as indicated. $^{*}p<0.05$, $^{**}p<0.01$, $^{****}p<0.0001$ (two-tailed unpaired t test) compared to the condition without 9-ING-41. Data shown as mean ± SD. gMFI, geometric mean fluorescence intensity; GSK-3β, glycogen synthase kinase-3 beta.

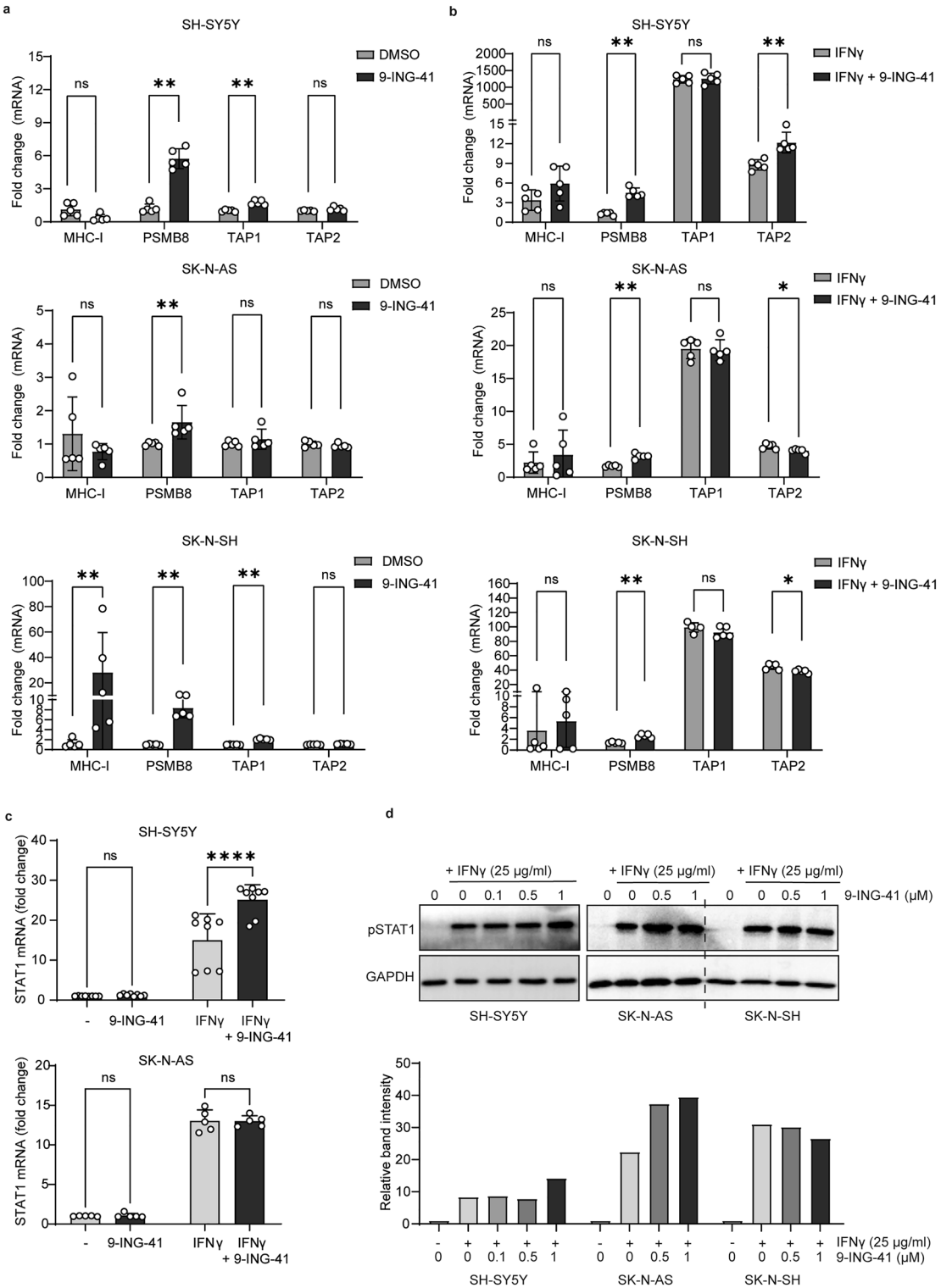

Fig. 3. 9-ING-41 can increase expression of genes involved in antigen processing and presentation in neuroblastoma cells (**a**, **b, c**) HLA-B, PSMB8, TAP1-2 and STAT1 mRNA were normalized to GAPDH and represented as fold change compared to the DMSO condition. Mann–Whitney U tests were used, where * < 0.05, ** $p < 0.01$, **** $p < 0.0001$. Data shown as mean ± SD. (**d**) Neuroblastoma cell lines were pre-treated for 30 min with the indicated concentrations of 9-ING-41 followed by 30 min of IFNγ. Protein expression was analyzed by Western Blotting on whole cell lysates. The original blot was cut above the 50 kDa mark. The upper part was then stained with an antibody against pSTAT1, while the lower part was stained with GAPDH loading control. An image was made from each of the two parts of the blot. The sections of interest were then cropped from the images and shown in the figure here. Full uncropped blots are shown in supplementary Fig. S4. pSTAT1, phosphorylated Signal Transducer And Activator Of Transcription 1; GAPDH, Glyceraldehyde 3-phosphate dehydrogenase; HLA-B, Human Leukocyte Antigen-B; PSMB8, proteasome 20S subunit B8; TAP1/2, Transporter Associated with antigen Processing 1/2.

9-ING-41 treatment of neuroblastoma cells potentiates activation and proliferation of human CTLs

We next asked whether GSK-3β inhibition in neuroblastoma cells potentiated the CTL-mediated immune response in line with the increased MHC-I display we observed. In addition to enhancing MHC-I surface display, IFNγ can upregulate PD-L1 expression on neuroblastoma cells[32,33]. As our STRING data base analysis (Fig. 2a) showed that GSK-3β can interact with PD-L1 (i.e., CD274), next we tested whether GSK-3β inhibition would affect PD-L1 expression on neuroblastoma cells. We cultured SH-SY5Y cells with 9-ING-41 and IFNγ for 72h and measured PD-L1 surface expression by flow cytometry. 9-ING-41 singular treatment had no significant effect on PD-L1 expression on neuroblastoma cells (Fig. 4b), but in combination with IFNγ did upregulate PD-L1 expression significantly compared to IFNγ alone (Fig. 4c). Therefore, we reasoned that anti-PD-1 treatment might be beneficial in combination with 9-ING-41 to promote neuroblastoma-induced CTL activation.

To assess this possibility, we made use of MHC-mismatch alloreactivity as readout for increased MHC-I-mediated immunogenicity and included anti-PD-1 treatment. We employed a mixed lymphocyte reaction protocol[34], that we modified to include neuroblastoma cells. We first pre-treated SH-SY5Y neuroblastoma cells with 9-ING-41 and irradiated the cells to prevent overgrowth. We then co-cultured the SH-SY5Y cells as antigen presenting cells with CD8 + T cells from an HLA-mismatching donor in presence of anti-CD28 antibodies, IL-2, and anti-PD-1 (Fig. 4a). The CD8 + T cells were isolated from healthy donor blood and stained with covalent amine-binding cell trace violet (CTV) to measure cell proliferation. After five days of co-culture, we measured the CD25 activation marker and proliferation of the CD8 + T cells by flow cytometry (gating strategy in supplemental Fig. S5). The CD8 + T cells co-cultured with 9-ING-41 pre-treated neuroblastoma cells expressed significantly higher levels of CD25 and Ki67 and proliferated significantly more compared to those co-cultured with DMSO control-treated SH-SY5Y cells (Fig. 4d–f). By itself, anti-PD-1 treatment of CD8 + T cells co-cultured with DMSO-treated neuroblastoma cells did not influence the measured activation and proliferation markers. Nonetheless, co-culture with 9-ING-41 pre-treated SH-SY5Y cells and anti-PD-1 triggered tenfold more CD8 + T cell proliferation and CD8 + T cell expansion, when compared to the anti-PD-1 condition. When IFNγ was included, differences were less pronounced, but the combination of 9-ING-41 pre-treated SH-SY5Y cells and anti-PD-1 significantly upregulated the CD25 cell surface expression and CD8 + T cell proliferation compared to control conditions where only IFNγ was added (Fig. 4g).

Overall, our data show that GSK-3β inhibition with 9-ING-41 can enhance expression of functional MHC-I on a subset of neuroblastoma cells and can potentiate their recognition by CTLs in an MHC mismatch-based culture system.

Discussion

9-ING-41 is currently, in 2024, an investigational small molecule inhibitor of GSK-3β in mid-stage clinical development in patients. A pre-clinical anti-tumor activity of the drug has been established in cell line and mouse models of neuroblastoma, with a hypothesized working mechanism of increasing apoptosis of cancer cells[18,35]. GSK-3β inhibition with 9-ING-41 has previously been shown to boost NK- and T-cell mediated killing of colorectal tumor cell lines[36]. Here, we investigated whether pharmacological inhibition of GSK-3β might increase the immunogenicity of neuroblastoma cells. Based on interplay between the GSK-3β pathway and the NFκB and IFNγ pathways, we hypothesized that GSK-3β inhibition might enhance the immunogenicity of neuroblastoma cells by amplifying MHC-I-mediated CD8 + T cell recognition. We found that 9-ING-41 can enhance MHC-I neuroblastoma cell surface display and expression of genes related to MHC-I APM pathway. Our results were most consistent in the non-MYCN-amplified cell lines. The enhanced MHC-I display potentiated the recognition of neuroblastoma cells by CD8 + T cells. Even though the MHC-I induction by the 9-ING-41 treatment alone might be considered modest, the CD8 + T cell reactivity increased significantly in response to the MHC-I induced by the 9-ING-41-treated neuroblastoma cells. As such, a relatively small but significant increase in MHC-I expression on the surface of neuroblastoma cells might trigger a protective anti-tumor response. In fact, engagement of one single TCR/CD3 might be sufficient to activate T cells[37]. To the best of our knowledge, our study is the first to report an immune stimulatory effect of 9-ING-41 directly on neuroblastoma cells.

As our protein–protein interaction analysis showed that GSK-3β can interact with proteins from the APM, we analyzed the gene expression of APM proteins following GSK-3β inhibition in neuroblastoma cells. Even though we observed significant differences in some of the genes tested, these differences were consistent among the cell lines only for the PSMB8 gene. We also observed that GSK-3β inhibition more consistently and significantly enhanced MHC-I protein levels compared to gene levels and thereby the effect on APM may also be more pronounced at the protein level, possibly affecting intracellular protein localization, stimulating peptide/MHC-I complex formation or transport to the cell surface. Indeed, 9-ING-41 inhibits the kinase activity of GSK-3β, further supporting an effect on protein level, but more experiments are needed to establish the mechanism(s) that drive the effect of GSK-3β inhibition on APM function. Further, we explored whether the 9-ING-41 partly acts through enhancement of IFNγ signaling, which, via stimulation of JAK/STAT1 signaling can also boosts MHC-I-mediated antigen presentation[4,27]. In support of this, we show that STAT1 protein phosphorylation is indeed enhanced in two of three neuroblastoma cell lines tested when GSK-3β is inhibited. This finding suggests that 9-ING-41 can amplify the effect of IFNγ on MHC-I expression in neuroblastoma cells. However, more in-depth pathway analysis is required to draw more definite conclusions on the interplay between GSK-3β inhibition and IFNγ signaling. Notably, IFNγ can be secreted in the microenvironment of neuroblastomas, for example by natural killer (NK) cells[28,29]. It is already shown that GSK-3β inhibition with CHIR99021 drives NK cell maturation and antitumor activity by increasing IFNγ secretion[38], a phenomenon currently exploited in the manufacturing of NK cell therapies. Therefore, GSK-3β inhibition may in fact have a dual role in enhancing CTL-mediated recognition and killing by directly stimulating the neuroblastoma cells to display MHC-I and

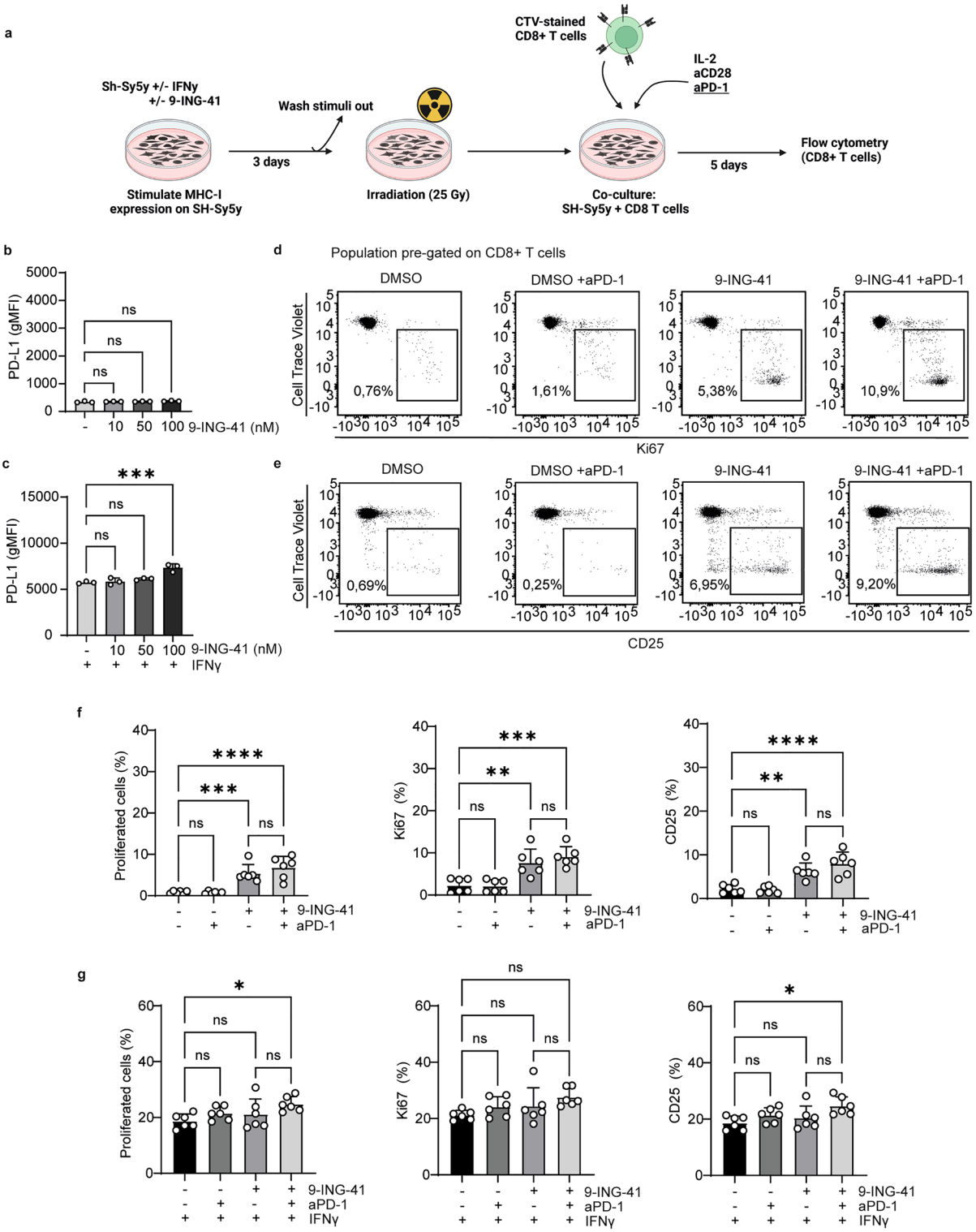

Fig. 4. 9-ING-41 in combination with anti-PD-1 therapy enhances immunogenicity of neuroblastoma cells (**a**) Experimental set-up of the CD8 + T cells-neuroblastoma co-culture. PD-L1 surface expression on neuroblastoma cells following treatment of increasing concentrations of 9-ING-41 without (**b**) or with (**c**) IFNγ. Expression measured by flow cytometry. (**d**) and (**e**) Representative plots of the flow cytometry staining for cell proliferation (CTV) and activation (CD25). Percentage proliferated (CTV negative), CD25 positive and Ki67 positive CD8 + T cells after co-culture with + /− 9-ING-41 pre-treated SH-Sy5y cells, without (**f**) or with (**g**) IFNγ. $^{*}p < 0.05$, $^{**}p < 0.01$, $^{***}p < 0.01$ using one-way ANOVA with Šidák correction for multiple comparisons. Data shown as mean ± SD. CD8 + T cells from three donors, conditions in duplicates. gMFI, geometric mean fluorescent intensity. CTV, cell trace violet.

express genes of key APM proteins, and by increasing the secretion of IFNγ by NK cells to indirectly enhance MHC-I display on the neuroblastoma cells.

Our initial database analysis revealed that that GSK-3β gene expression in tumors reversely correlates with survival, especially for patients with neuroblastomas without MYCN amplification. In line with this, the observed effect of GSK-3β inhibition on MHC-I display was most pronounced on the cells without MYCN amplification. While SK-N-SH cell are considered non-MYCN-amplified, we observed a higher expression of MYCN in SK-N-SH compared to the other non-MYCN-amplified cell lines. The higher expression of MYCN in SK-N-SH cells may underscore the decreased effect of 9-ING-41 on MHC-I expression and IFNγ signaling in this cell line. While these data indicate a potential link between MYCN amplification and GSK-3β expression, in our experiments, MYCN exogenous overexpression in SH-SY5Y cells did not genetically reprogram the GSK-3β expression. In healthy humans, MYCN is expressed only in certain embryonal tissues, and in adult cells its expression is very low or missing[39]. The functioning of endogenous, overexpressed, and amplified MYCN can have different impacts on the cell fate decisions[40], suggesting that our MYCN overexpression system cannot mimic the physiological effects of MYCN amplification on GSK-3β expression. Future studies should identify the effects of MYCN amplification on GSK-3β expression as well as on the sensitivity of GSK-3β inhibition. Thus, we can improve the stratification of the patient groups that would benefit most from 9-ING-41 therapy.

In this preclinical study, we used in vitro neuroblastoma models, which evidently has limitations compared to in vivo studies. Further, even though we show that 9-ING-41 boosts the expression of functional MHC-I on neuroblastoma cells and T cells respond to the MHC-I mismatch, we do not show direct TCR-driven recognition and killing of the tumor cells. A model to determine antigen-specific T cell killing of neuroblastoma cells can further corroborate the importance of modest increases in MHC-I expression on the neuroblastoma cells in T cell recognition and killing. Nonetheless, based on what is known in literature about the specificity and function of 9-ING-41, together with the novel insights into its immunogenic effects provided here, we propose that this study may help advance clinical studies of 9-ING-41 for neuroblastoma treatment. 9-ING-41 has recently entered clinical trials for adult patients with advanced refractory cancer, where it shows established efficacy and a favorable safety profile[20,41]. Overall, our results provide evidence for the rationale to include patients with neuroblastoma in clinical trials for 9-ING-41 as adjuvant treatment to already existing immunotherapies.

Methods

Cell culture

The neuroblastoma cell lines were obtained from Princes Maxima Center, Utrecht, the Netherlands. The cell lines were cultured in DMEM GlutaMAX (ThermoFisher Scientific) supplemented with 10% fetal calf serum (FCS), 1% penicillin–streptomycin (Merck Life Sciences), 1 × MEM non-essential amino acids (Gibco).

For the T cell isolation, peripheral blood was collected from healthy subjects into BD Vacutainer blood collection tubes with sodium heparin. The healthy subjects have signed informed consent for research purposes (Mini Donor Dienst, UMC Utrecht, the Netherlands). Peripheral blood mononuclear cells were isolated with Ficoll-Paque density gradient centrifugation. CD8 + T cells were isolated using the CD8 T cell isolation kit (Miltenyi) with autoMACS automated cell isolation following the manufacturer's protocol. CD8 + T cells were cultured in RPMI 1640 (ThermoFisher Scientific) supplemented with 10% FCS, 1% penicillin–streptomycin. CD28 Monoclonal Antibody (CD28.2) (AntibodyChain International; 1 mg/ml), recombinant human IL-2 (Novartis; 10 IU/ml) and Pembrolizumab anti-PD-1 (KEYTRUDA®, 10 mg/ml) were used for the neuroblastoma-CD8 + T cell co-culture.

Flow cytometry

Cells were washed twice with FACS buffer (PBS supplemented with 2% FBS and 0.1% sodium azide) followed by incubation with 10% mouse serum in FACS buffer to prevent nonspecific binding. After staining with Fixable Viability dye eFluor 507 (eBioscience) in PBS the cells were stained with surface antibodies MHC-1, PD-L1, CD8 and CD3 in FACS buffer. In case of intracellular stainings, the cells were fixed and permeabilized using Fixation and Permeabilization buffer (eBioscience) and subsequently stained with Ki-67 antibody. The antibodies used are described in supplemental table S1. Following the staining, cells were washed twice and taken up in FACS buffer for measurement on the BD LSR Fortessa with FACSDiva software. Analysis was performed with Flowjo (V.10.5.3).

Quantitative real-time PCR

Total cellular RNA was extracted using the RNeasy mini kit (Qiagen) according to the manufacturer's protocol. For each sample, the same amount of RNA was transcribed into cDNA with the cDNA Synthesis Kit (Bio-Rad). For the quantitative real-time PCR (qRT-PCR) we used SYBR green qPCR master mix (Bio-Rad) and primers listed in supplemental table S2. The qRT-PCR reaction was carried out using a Quantstudio 3 apparatus (Bio-Rad). We used GAPDH as endogenous control.

Analysis of patient cohorts from online datasets

For the survival analysis and GSK-3β expression analysis, the data was generated from the R2 Genomic Analysis and Visualization Platform (http://r2.amc.nl) and the cBioPortal for cancer genomics (https://www.cbioportal.org/). Kaplan–Meier estimates of overall survival were determined using automatically generated expression cutoff values based on statistically significant differences using log-rank test.

Immunoblotting

We lysed the cells in commercially obtained RIPA buffer (Sigma) in presence of Halt™ Protease Inhibitor Cocktail (ThermoFisher) followed by boiling (10 min at 95 °C). Cell lysates were run on SDS-PAGE and transferred onto polyvinylidene fluoride (PVDF) membrane (Merck Millipore). We blocked the membranes with 5% milk powder (Campina) in PBS 0.1% Tween-20 for 1 h before probing with the specific primary antibodies (16 h at 4 °C). Subsequently, we washed and stained the membranes with HRP-coupled secondary antibodies for 1 h. We analyzed the images on ChemiDoc Imaging System (Bio-Rad).

Statistical analysis

Variables are presented as mean and standard deviation. Two-tailed unpaired t test or Mann–Whitney U tests were used when comparing two groups. One-way ANOVA with Šidák correction or Dunnett's multiple comparison was used when comparing more than two groups. Log rank tests for Kaplan–Meier survival data were performed to determine significant differences. All statistical analysis were performed using GraphPad Prism (V.8.3.0). $P < 0.05$ was considered statistically significant.

Data availability

All data generated or analysed during this study are included in this published article (and its Supplementary Information files).

Received: 10 June 2024; Accepted: 9 September 2024
Published online: 17 September 2024

References

1. Croteau, N., Nuchtern, J. & LaQuaglia, M. P. Management of neuroblastoma in pediatric patients. *Surg. Oncol. Clin. North Am.* **30**, 291–304. https://doi.org/10.1016/j.soc.2020.11.010 (2021).
2. Anderson, J., Majzner, R. G. & Sondel, P. M. Immunotherapy of neuroblastoma: Facts and hopes. *Clin. Cancer Res.* **28**, 3196–3206. https://doi.org/10.1158/1078-0432.CCR-21-1356 (2022).
3. Yarmarkovich, M. *et al.* Targeting of intracellular oncoproteins with peptide-centric CARs. *Nature* **623**, 820–827 (2023).
4. Spel, L. *et al.* Natural killer cells facilitate PRAME-specific T-cell reactivity against neuroblastoma. vol. 6 www.impactjournals.com/oncotarget.
5. Dhatchinamoorthy, K., Colbert, J. D. & Rock, K. L. Cancer immune evasion through loss of MHC class I antigen presentation. *Front. Immunol* **12**, 636568. https://doi.org/10.3389/fimmu.2021.636568 (2021).
6. Balasubramanian, A., John, T. & Asselin-Labat, M. L. Regulation of the antigen presentation machinery in cancer and its implication for immune surveillance. *Biochem. Soc. Trans.* **50**, 825–837. https://doi.org/10.1042/BST20210961 (2022).
7. Burr, M. L. *et al.* An evolutionarily conserved function of polycomb silences the MHC class I antigen presentation pathway and enables immune evasion in cancer. *Cancer Cell* **36**, 385-401.e8 (2019).
8. Chen, C. L. *et al.* Role of glycogen synthase kinase-3 in interferon-γ-mediated immune hepatitis. *Int. J. Mol. Sci.* **23**, 4669. https://doi.org/10.3390/ijms23094669 (2022).
9. Kai, J. I. *et al.* Glycogen synthase kinase-3β indirectly facilitates interferon-γ-induced nuclear factor-κB activation and nitric oxide biosynthesis. *J. Cell Biochem.* **111**, 1522–1530 (2010).
10. Tsai, C.-C. *et al.* Glycogen synthase kinase-3β facilitates IFN-γ-induced STAT1 activation by regulating Src homology-2 domain-containing phosphatase 2. *J. Immunol.* **183**, 856–864 (2009).
11. Medunjanin, S. *et al.* GSK-3β controls NF-kappaB activity via IKKγ/NEMO. *Sci. Rep.* **6**, 38553 (2016).
12. Abd-Ellah, A., Voogdt, C., Krappmann, D., Möller, P. & Marienfeld, R. B. GSK3β modulates NF-κB activation and RelB degradation through site-specific phosphorylation of BCL10. *Sci. Rep.* **8**, 1352 (2018).
13. Spel, L., Schiepers, A. & Boes, M. NFκB and MHC-1 interplay in neuroblastoma and immunotherapy. *Trends Cancer* **4**, 715–717. https://doi.org/10.1016/j.trecan.2018.09.006 (2018).
14. Spel, L. *et al.* Nedd4-binding protein 1 and TNFAIP3-interacting protein 1 control MHC-1 display in neuroblastoma. *Cancer Res.* **78**, 6621–6631 (2018).
15. Korur, S. *et al.* GSK3β regulates differentiation and growth arrest in glioblastoma. *PLoS One* **4**, e7443 (2009).
16. Becker, M. *et al.* Polycomb protein BMI1 regulates osteogenic differentiation of human adipose tissue-derived mesenchymal stem cells downstream of GSK3. *Stem Cells Dev.* **25**, 922–933 (2016).
17. Duda, P. *et al.* Targeting GSK3 and associated signaling pathways involved in cancer. *Cells* **9**, 1110. https://doi.org/10.3390/cells9051110 (2020).
18. Ugolkov, A. V. *et al.* 9-ING-41, a small-molecule glycogen synthase kinase-3 inhibitor, is active in neuroblastoma. *Anticancer Drugs* **29**, 717–724 (2018).
19. Anraku, T. *et al.* Clinically relevant GSK-3β inhibitor 9-ING-41 is active as a single agent and in combination with other antitumor therapies in human renal cancer. *Int. J. Mol. Med.* **45**, 315–323 (2020).
20. Hsu, A. *et al.* Clinical activity of 9-ING-41, a small molecule selective glycogen synthase kinase-3 beta (GSK-3β) inhibitor, in refractory adult T-Cell leukemia/lymphoma. *Cancer Biol. Ther.* **23**, 417–423 (2022).
21. Park, R., Coveler, A. L., Cavalcante, L. & Saeed, A. Gsk-3β in pancreatic cancer: Spotlight on 9-ing-41, its therapeutic potential and immune modulatory properties. *Biology* **10**, 610. https://doi.org/10.3390/biology10070610 (2021).
22. de Bruijn, I. *et al.* Analysis and visualization of longitudinal genomic and clinical Data from the AACR project GENIE biopharma collaborative in cBioPortal. https://doi.org/10.1158/0008-5472.CAN-23-0816/3362081/can-23-0816.pdf.
23. Cerami, E. *et al.* The cBio cancer genomics portal: An open platform for exploring multidimensional cancer genomics data. *Cancer Discov.* **2**, 401–404 (2012).
24. Gao, J. *et al.* Integrative analysis of complex cancer genomics and clinical profiles using the CBioPortal InTRODUcTiOn EQUiP-MenT InSTRUcTiOnS querying individual cancer studies viewing and interpreting the results performing cross-cancer queries viewing cancer study summary data viewing genomic alterations in a single tumor: Patient view programmatic access notes and remarks complementary data sources and analysis Options future directions. vol. 6 http://www.adobe.com/products/illustrator.html (2013).
25. Ghandi, M. *et al.* Next-generation characterization of the cancer cell line encyclopedia. *Nature* **569**, 503–508 (2019).
26. Wienke, J. *et al.* The immune landscape of neuroblastoma: Challenges and opportunities for novel therapeutic strategies in pediatric oncology. *Eur. J. Cancer* **144**, 123–150. https://doi.org/10.1016/j.ejca.2020.11.014 (2021).
27. Zhou, F. Molecular mechanisms of IFN-γ to up-regulate MHC class I antigen processing and presentation. *Int. Rev. Immunol.* **28**, 239–260. https://doi.org/10.1080/08830180902978120 (2009).

28. Bottino, C. *et al.* Natural killer cells and neuroblastoma: Tumor recognition, escape mechanisms, and possible novel immunotherapeutic approaches. *Front. Immunol.* **5**, 56. https://doi.org/10.3389/fimmu.2014.00056 (2014).
29. Neal, Z. C. *et al.* NXS2 murine neuroblastomas express increased levels of MHC class I antigens upon recurrence following NK-dependent immunotherapy. *Cancer Immunol. Immunother.* **53**, 41–52 (2004).
30. Kaya, Z. B. *et al.* Optimizing SH-SY5Y cell culture: exploring the beneficial effects of an alternative media supplement on cell proliferation and viability. *Sci. Rep.* **14**, 4775 (2024).
31. Kovalevich, J. & Langford, D. Considerations for the use of SH-SY5Y neuroblastoma cells in neurobiology. *Methods Mol. Biol.* **1078**, 9–21 (2013).
32. Zhao, T., Li, Y., Zhang, J. & Zhang, B. Pd-l1 expression increased by ifn-γ via jak2-stat1 signaling and predicts a poor survival in colorectal cancer. *Oncol. Lett.* **20**, 1127–1134 (2020).
33. Garcia-Diaz, A. *et al.* Interferon receptor signaling pathways regulating PD-L1 and PD-L2 expression. *Cell. Rep.* **19**, 1189–1201 (2017).
34. Nguyen, X. D. *et al.* Flow cytometric analysis of T cell proliferation in a mixed lymphocyte reaction with dendritic cells. *J. Immunol. Methods* **275**, 57–68 (2003).
35. Dickey, A. *et al.* GSK-3β inhibition promotes cell death, apoptosis, and in vivo tumor growth delay in neuroblastoma Neuro-2A cell line. *J. Neurooncol.* **104**, 145–153 (2011).
36. Huntington, K. E., Zhang, S., Carneiro, B. A. & El-Deiry, W. S. Abstract 2676: GSK3β inhibition by small molecule 9-ING-41 decreases VEGF and other cytokines, and boosts NK and T cell-mediated killing of colorectal tumor cells. *Cancer Res.* **81**, 2676 (2021).
37. Gudipati, V. *et al.* Inefficient CAR-proximal signaling blunts antigen sensitivity. *Nat. Immunol.* **21**, 848–856 (2020).
38. Cichocki, F. *et al.* GSK3 inhibition drives maturation of NK cells and enhances their antitumor activity. *Cancer Res.* **77**, 5664–5675 (2017).
39. Hirvonen, H. *et al.* The N-Myc Proto-Oncogene and IGF-II Growth Factor MRNAs Are Expressed by Distinct Cells in Human Fetal Kidney and Brain. http://rupress.org/jcb/article-pdf/108/3/1093/1462919/1093.pdf.
40. Duffy, D. J. *et al.* Integrative Omics Reveals MYCN as a Global Suppressor of Cellular Signalling and Enables Network-Based Therapeutic Target Discovery in Neuroblastoma. vol. 6 www.impactjournals.com/oncotarget.
41. Odia, Y. *et al.* Malignant glioma subset from actuate 1801: Phase I/II study of 9-ING-41, GSK-3β inhibitor, monotherapy or combined with chemotherapy for refractory malignancies. *Neurooncol Adv* **4**, (2022).

Author contributions

AM and MB initiated the study. AM performed the experiments and data analyses. AM and KS performed the survival analysis from the online repositories. JM performed the STRING analysis. APM and DMS provided 9-ING-41 reagent for experimental use. All authors contributed to substantial discussion of content, reviewed, and approved the final manuscript.

Funding

This research was funded by a non-restricted grant from Actuate Therapeutics. The funder had no role in study design.

Competing interests

This study was paid by a research grant from Actuate Therapeutics (MB). MB also received funding from Nutricia and Argenx, unrelated to the submitted work. APM and DMS work for Actuate Therapeutics. All other authors state no conflict of interest and have no disclosures.

Additional information

Supplementary Information The online version contains supplementary material available at https://doi.org/10.1038/s41598-024-72492-y.

Correspondence and requests for materials should be addressed to M.B.

Reprints and permissions information is available at www.nature.com/reprints.

Publisher's note Springer Nature remains neutral with regard to jurisdictional claims in published maps and institutional affiliations.